

# Emergence of brain-derived neurotrophic factor-induced postsynaptic potentiation of NMDA currents during the postnatal maturation of the Kölliker–Fuse nucleus of rat

Miriam Kron<sup>1,3</sup>, Julia Reuter<sup>1</sup>, Ellen Gerhardt<sup>2</sup>, Till Manzke<sup>1,2</sup>, Weiqi Zhang<sup>1,2</sup> and Mathias Dutschmann<sup>1,3</sup>

<sup>1</sup>Department of Neuro and Sensory Physiology, University Medicine Göttingen, Georg August University, Humboldtallee 23, 37073 Göttingen, Germany

<sup>2</sup>Deutsche Forschungsgemeinschaft Research Center for Molecular Physiology of the Brain (CMPB), 37073 Göttingen, Germany

<sup>3</sup>Bernstein Center for Computational Neurosciences (BCCN), 37073 Göttingen, Germany

The Kölliker–Fuse nucleus (KF) contributes essentially to respiratory pattern formation and adaptation of breathing to afferent information. Systems physiology suggests that these KF functions depend on NMDA receptors (NMDA-R). Recent investigations revealed postnatal changes in the modulation of glutamatergic neurotransmission by brain-derived neurotrophic factor (BDNF) in the KF. Therefore, we investigated postnatal changes in NMDA-R subunit composition and postsynaptic modulation of NMDA-R-mediated currents by BDNF in KF slice preparations derived from three age groups (neonatal: postnatal day (P) 1–5; intermediate: P6–13; juvenile: P14–21). Immunohistochemistry showed a developmental up-regulation of the NR2D subunit. This correlated with a developmental increase in decay time of NMDA currents and a decline of desensitization in response to repetitive exogenous NMDA applications. Thus, developmental up-regulation of the NR2D subunit, which reduces the Mg<sup>2+</sup> block of NMDA-R, causes these specific changes in NMDA current characteristics. This may determine the NMDA-R-dependent function of the mature KF in the control of respiratory phase transition. Subsequent experiments revealed that bath-application of BDNF progressively potentiated these repetitively evoked NMDA currents only in intermediate and juvenile age groups. Pharmacological inhibition of protein kinase C (PKC), as a downstream component of the BDNF–tyrosine kinase B receptor (trkB) signalling, prevented BDNF-induced potentiation of NMDA currents. BDNF-induced potentiation of NMDA currents in later developmental stages might be essential for synaptic plasticity during the adaptation of the breathing pattern in response to peripheral/central commands. The lack of plasticity in neonatal neurones strengthens the hypothesis that the respiratory network becomes permissive for activity-dependent plasticity with ongoing postnatal development.

(Received 27 November 2007; accepted after revision 3 March 2008; first published online 13 March 2008)

**Corresponding author** M. Dutschmann: Department of Neuro and Sensory Physiology, University Medicine Göttingen, Georg August University, Humboldtallee 23, 37073 Göttingen, Germany. Email: mdutsch@gwdg.de

The Kölliker–Fuse nucleus (KF) within the dorsolateral pons is an essential part of the respiratory network (St-John, 1998; Alheid *et al.* 2004; Ezure, 2004; Dutschmann & Herbert, 2006). In the absence of afferent feedback from pulmonary stretch receptors, the KF is crucially involved in *N*-methyl-D-aspartate receptor (NMDA-R)-dependent mediation of inspiratory/expiratory phase transition of the respiratory cycle (Bianchi *et al.* 1995; Bonham, 1995; St-John, 1998). Importantly, the KF receives second order synaptic inputs from somato- (e.g. spinal trigeminal tract; Feil & Herbert,

1995) and viscerosensory relays (e.g. the nucleus of solitary tract (NTS); Herbert *et al.* 1990). Thus, it is involved in the adaptation of the breathing pattern in response to various kinds of afferent information. During the processing of afferent information, NMDA-R again may play a dominant role (Dutschmann & Herbert, 1998; Dutschmann *et al.* 1998; Siniaia *et al.* 2000; Okazaki *et al.* 2002; Takano & Kato, 2003; Dutschmann *et al.* 2004; Song & Poon, 2004). Since glutamatergic neurotransmission via NMDA-R is linked to synaptic plasticity (Sheng & Kim, 2002), it is not surprising that KF-mediated plasticity apparently depends on neurotransmission via NMDA-R (Dutschmann *et al.* 2004; Song & Poon, 2004). NMDA-R-mediated plasticity is linked to NMDA-R

This paper has online supplemental material.

**Table 1. Developmental changes in NR2B and NR2D expression in selected nuclei of the respiratory network**

NR2B					
Age	VRG	preBötC	pFRG	A5	KF
P1/P2 ( <i>n</i> = 4)	80.8 ± 8.8	34.3 ± 4.4	16.3 ± 1.7	34.3 ± 4.9	37.0 ± 6.6
P4/P5 ( <i>n</i> = 3)	63.3 ± 9.7	45.3 ± 6.1	14.7 ± 0.9	31.0 ± 4.0	33.0 ± 5.0
P7/P8 ( <i>n</i> = 4)	33.0 ± 6.0	28.8 ± 3.7	7.0 ± 0.9	20.3 ± 2.7	27.3 ± 1.3
P10/P12 ( <i>n</i> = 4)	13.5 ± 1.9	17.3 ± 1.1	7.5 ± 1.0	16.5 ± 1.0	16.8 ± 1.3
P14/P16 ( <i>n</i> = 4)	15.3 ± 6.7	10.3 ± 0.8	5.5 ± 1.0	9.3 ± 1.5	13.8 ± 1.1
P18/P21 ( <i>n</i> = 4)	8.0 ± 0.7	6.0 ± 0.7	4.8 ± 1.1	7.5 ± 0.6	17.0 ± 1.2
NR2D					
P1/P2 ( <i>n</i> = 4)	72.8 ± 7.3	23.8 ± 5.9	12.8 ± 1.0	30.0 ± 2.3	9.0 ± 0.0
P4/P5 ( <i>n</i> = 3)	40.0 ± 12.5	19.3 ± 4.2	11.0 ± 2.5	18.0 ± 4.5	8.0 ± 0.6
P7/P8 ( <i>n</i> = 4)	24.0 ± 3.3	15.3 ± 1.3	7.0 ± 0.4	8.3 ± 0.5	10.0 ± 1.3
P10/P12 ( <i>n</i> = 4)	16.0 ± 1.2	8.3 ± 0.8	6.3 ± 0.9	11.5 ± 3.9	17.0 ± 1.4
P14/P16 ( <i>n</i> = 4)	10.3 ± 0.9	7.0 ± 0.8	6.8 ± 0.9	8.5 ± 0.5	17.8 ± 2.6
P18/P21 ( <i>n</i> = 4)	7.3 ± 0.9	8.0 ± 0.7	6.3 ± 0.3	7.3 ± 1.0	28.8 ± 4.0

Numbers represent means ± s.e.m. of NR2B- and NR2D-positive cells within 10 000  $\mu\text{m}^2$  of each region. KF, Kölliker–Fuse nucleus; pFRG, parafacial respiratory group; pre-BötC, pre-Bötzinger complex; VRG, ventral respiratory group.

subunit composition (Monyer *et al.* 1994; Cull-Candy *et al.* 2001) and also involves intracellular signalling pathways, which are activated either directly by  $\text{Ca}^{2+}$  influx or secondarily by the release of neuromodulators. One of these neuromodulators is brain-derived neurotrophic factor (BDNF), acting on tyrosine kinase B receptor (trkB) which can induce a rapid phosphorylation of different NMDA-R subunits (Suen *et al.* 1997; Lin *et al.* 1998; Slack *et al.* 2004). This, in turn, modulates NMDA-R conductance (Levine *et al.* 1998; Yamada *et al.* 2002; Kim *et al.* 2006; Xu *et al.* 2006) and is linked to learning and memory processes (Lu, 2003). A recent publication showed that BDNF becomes a potent modulator of glutamatergic neurotransmission during the postnatal ontogeny of the KF (Kron *et al.* 2007a). Thereby, BDNF is potentially released in the KF via pathways arising from the NTS, which densely expresses BDNF (Wang *et al.* 2006).

Importantly, the KF is immature at birth. Previous studies demonstrated that the postnatal maturation of the KF is reflected in changes of morphological and synaptic properties (Dutschmann *et al.* 2004; Kron *et al.* 2007a,b). These developmental changes are most likely also associated with the NMDA-R-dependent processing of afferent inputs which are silent or not functional prenatally. Interestingly, the adult KF contains high mRNA levels for the NMDA-R subunit 2D (NR2D, Guthmann & Herbert, 1999), whereas in other brain regions the NR2D subunit is down-regulated during postnatal development (Akazawa *et al.* 1994; Monyer *et al.* 1994; Cull-Candy *et al.* 2001). This implicates a different developmental course of NR2D expression in the KF. However, the developmental changes of NR2D subunit expression until now have not been investigated.

The present study investigated developmental changes in: (i) NMDA-R subunit NR2D expression, (ii) NMDA current characteristics and (iii) postsynaptic modulation of NMDA currents by BDNF in the developing KF. We show that developmental up-regulation of the NMDA-R subunit NR2D corresponds with an increasing decay time of NMDA currents and a lack of desensitization. Furthermore, BDNF caused a progressive potentiation of NMDA currents in the juvenile KF. The BDNF-evoked potentiation could be blocked by inhibition of protein kinase C (PKC), a downstream component in trkB-mediated signalling pathways, and by the chelation of intracellular  $\text{Ca}^{2+}$  with BAPTA.

## Methods

### Immunohistochemistry

All experiments were performed in accordance with the ethical guidelines of the U.S. National Institutes of Health (NIH) and were approved by the ethics committee of the University Medical Center Göttingen, Georg-August-University.

To investigate developmental changes in the distribution of the NMDA-R subunit 2B (NR2B) and NR2D in the brainstem, immunofluorescence studies were performed. Sprague–Dawley rats of both sexes (*n* = 23) between P1 and P21 (details see Table 1) were deeply anaesthetized with isoflurane (1-chloro-2,2,2-trifluoroethyl-difluoromethylether; Abbott, Wiesbaden, Germany). Once respiration was depressed severely and the animals failed to respond to noxious pinch of tail or toe, the thorax was opened and the animals were

perfused transcardially with ice-cold phosphate-buffered saline (PBS) followed by 150–250 ml ice-cold 4% paraformaldehyde (PFA) in PBS. Brains were removed and post-fixed in 4% PFA containing 30% sucrose (neoLab, Heidelberg, Germany) for at least 48 h until processing.

The brainstems were dissected and cut into consecutive coronal sections (40  $\mu\text{m}$ ) using a freezing microtome (Reichert and Jung, Germany). Sections were collected in PBS and divided in three series, two for immunofluorescence stainings (free floating) for NR2B and NR2D and the adjacent section for thionin staining to compare the expression patterns with the specific anatomy of nuclei of the ponto-medullary respiratory network.

For permeabilization of the tissue, sections for immunofluorescence were rinsed several times in PBS and afterwards transferred into PBS containing 0.2% Triton X-100 (Sigma, Steinheim, Germany) for 10–45 min depending on age. The shorter times for permeabilization were used for neonatal tissue.

To reduce non-specific binding of the secondary antibody, all sections were later incubated in 2% bovine serum albumin (BSA; Carl Roth, Karlsruhe, Germany) diluted in PBS. After these initial procedures the sections were incubated with a goat anti-NR2B polyclonal antibody (Santa Cruz, Heidelberg, Germany; 4  $\mu\text{g ml}^{-1}$  in 2% BSA) or rabbit anti-NR2D polyclonal antibody (Santa Cruz; 2  $\mu\text{g ml}^{-1}$  in 2% BSA) for 1 h at room temperature followed by 16–20 h at 4°C. After rinsing in PBS, sections were incubated with the secondary chicken anti-goat antibody, conjugated to Alexa Fluor 488 (10  $\mu\text{g ml}^{-1}$ ; Invitrogen, Karlsruhe, Germany) for NR2B or donkey anti-rabbit conjugated to Alexa Fluor 555 (10  $\mu\text{g ml}^{-1}$ , Invitrogen) for NR2D for 2.5 h at room temperature. Sections were washed again, mounted on gelatine-coated slides, allowed to dry overnight and coverslipped with fluorescence mounting medium (Dako, Hamburg, Germany). For both antibodies, the specificity was tested (see online Supplemental material).

### Electrophysiological recordings

Sprague–Dawley rats of different ages (P1–21, either sex) were anaesthetized deeply with isoflurane until no reflex response to noxious pinch in toe or tail was observed. The animals were decapitated during anaesthesia, brains were removed and the ponto-medullary brainstem was transected. The brainstem was cut into 200–250  $\mu\text{m}$  sections using a vibratome (752M vibroslice, Campden Instruments, Loughborough, UK). Preparation of slices was performed in ice-cold artificial cerebrospinal fluid (ACSF) containing (mM): NaCl 125, KCl 3,  $\text{KH}_2\text{PO}_4$  1.25,  $\text{CaCl}_2$  2.5,  $\text{MgSO}_4$  1.25,  $\text{NaHCO}_3$  25, D-glucose 10 (all Sigma, Steinheim, Germany). ACSF was equilibrated to pH 7.4 with carbogen (95%  $\text{O}_2$ –5%  $\text{CO}_2$ ). All slices were incubated for at least 30 min

in oxygenated 35°C ACSF. Slices were transferred into oxygenated ACSF at room temperature and kept for up to 7 h. For some experiments, slices were incubated with the calcium chelator BAPTA-AM (1,2-bis(2-aminophenoxy)ethane-*N,N,N',N'*-tetraacetic acid tetrakis-(acetoxymethyl) ester; Sigma; 25  $\mu\text{M}$  for 1 h) to buffer fast intracellular  $\text{Ca}^{2+}$  elevations. For recording, slices were placed in a recording chamber, held in place with a platinum-wired nylon grid, and continuously superfused at 28°C with oxygenated ACSF.

The KF was identified ventral to the tip of the superior cerebellar peduncle (scp; see Fig. 1). In neonatal slices (< P3), the scp is barely detectable. Therefore, in neonatal slices we determined the KF region according to its presumed position between the mesencephalic trigeminal nucleus (Me5), the principal sensory trigeminal nucleus (Pr5) and the motor trigeminal nucleus (5N) as described previously (for details see Kron *et al.* 2007a).

Voltage clamp recordings were performed at a holding potential of –40 mV to reduce the  $\text{Mg}^{2+}$  block. To block action potential-dependent activity, 0.5  $\mu\text{M}$  tetrodotoxin (TTX; Alomone, Jerusalem, Israel) was included in the bath solution. The intracellular solution contained (mM): potassium gluconate 140,  $\text{CaCl}_2$  1, ethylene glycol-bis(2-aminoethylether)-*N,N,N',N'*-tetraacetic acid (EGTA) 10,  $\text{MgCl}_2 \cdot 6\text{H}_2\text{O}$  2,  $\text{Na}_2\text{GTP}$  0.5,  $\text{Na}_2\text{ATP}$  4, Hepes 10 (all Sigma). In some experiments the protein kinase C inhibitor peptide [19–36] (1  $\mu\text{M}$ ; Calbiochem, Darmstadt, Germany) was added to the intracellular solution to block PKC activity.

*N*-Methyl-D-aspartic acid (NMDA) currents were obtained by pressure ejection (5–10 ms) of NMDA (10 mM; Sigma) via a manually trimmed application pipette. One recording trial consisted of five consecutive NMDA applications with an interval of 15 s. The pressure for the ejection was adjusted until the threshold for NMDA-evoked currents was reached. For recordings, a pressure twofold over the threshold was used. To further reduce technical variation, tip diameter of the injection pipettes (~50  $\mu\text{m}$ ) and the distance to the recorded neurone (~50–100  $\mu\text{m}$ ) were kept constant throughout experiments. Finally, all analysed currents were derived from means of five consecutive NMDA applications (15 s interval) to further reduce variability caused by the technical setup.

Data were acquired using pCLAMP acquisition software (v. 9.2, Axon Instruments/Molecular Devices). Signals were amplified (Multiclamp 700B, Axon Instruments/Molecular Devices), filtered at 1 kHz, and digitized at 10 kHz.

### Experimental protocols

To test the effects of BDNF on NMDA currents, the experiments were performed in four consecutive

trials (5 repetitive ejections per trial, 15 s intervals). The first trial always reflected the control ( $t = 0$  min) while the subsequent ejections were performed 2 min ( $t = 2$  min), 10 min ( $t = 10$  min) and 20 min ( $t = 20$  min) after effective bath application of BDNF (excluding dead space circulation). Physiological quantities of BDNF peak around  $1 \text{ ng (g tissue)}^{-1}$  in the cortex (Das *et al.* 2001; Gilmore *et al.* 2003). Dose–response curves of BDNF effects on spontaneous postsynaptic currents revealed effective concentrations in the picomolar range (for details, see Kron *et al.* 2007a). Therefore, BDNF (Calbiochem)

was bath-applied at a concentration of  $50 \text{ pM}$  which corresponds to  $1.4 \text{ ng ml}^{-1}$  in the superfusate. As BDNF may have long-term effects, each slice was exposed to BDNF only once.

### Data analysis

Fluorescence-labelled neurones were documented with a Zeiss LSM 510 META confocal microscope (Oberkochen, Germany). The developmental expression patterns of NR2B and NR2D were analysed within selected nuclei

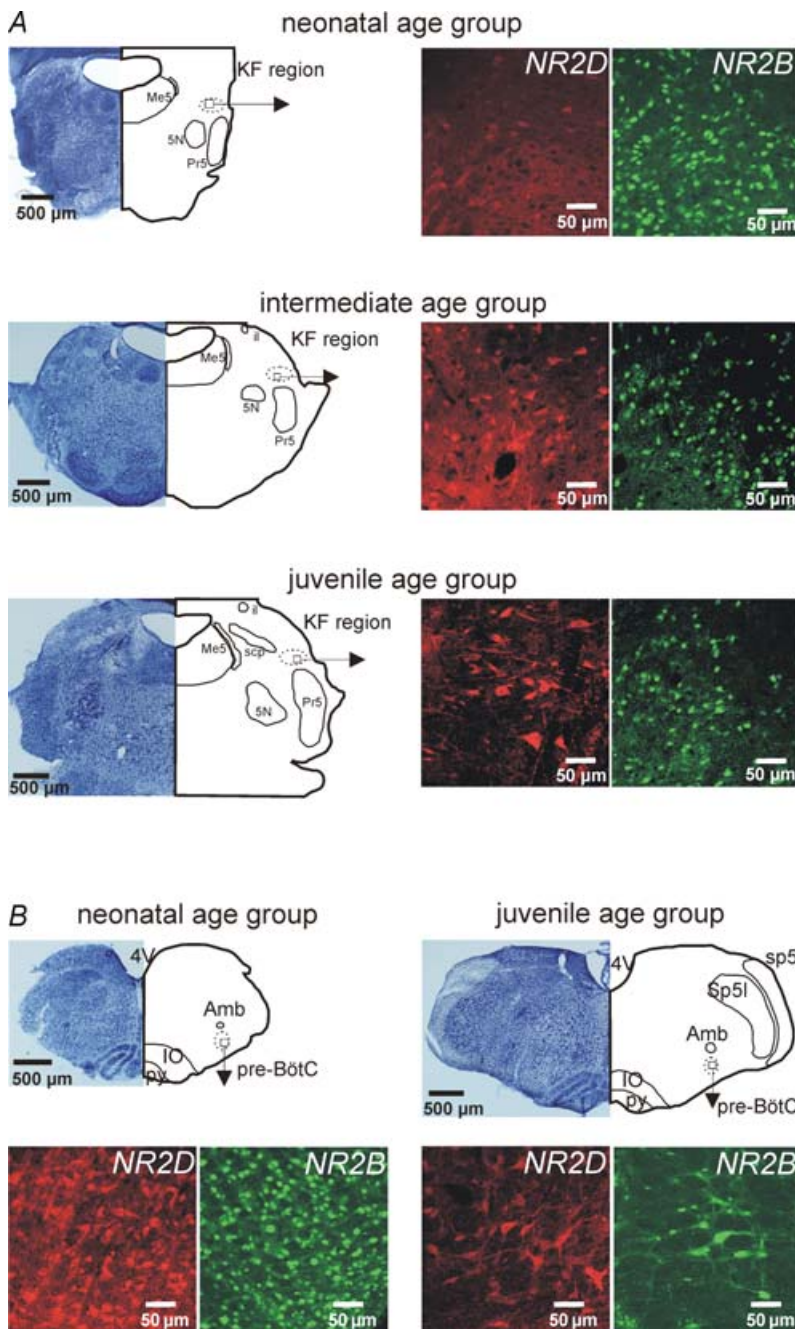


**Figure 1. Developmental changes in the expression pattern of the NR2D and NR2B subunit in the KF and pre-BötC**

A, photomicrographs illustrate developmental changes in the expression profile of NMDA receptor subunits in the KF. NR2D shows a developmental up-regulation while NR2B displays a developmental down-regulation. B, documentation of a developmental down-regulation of both NR2D and NR2B subunit expression in the pre-Bötzing complex (pre-BötC). Abbreviations: 4V, 4th ventricle; 5N, trigeminal motor nucleus; Amb, nucleus ambiguus; il, internal lateral subnucleus of the parabrachial complex; IO, inferior olive; KF, Kölliker–Fuse nucleus; Me5, mesencephalic nucleus of the trigeminus; Pr5, principal nucleus of trigeminal tract; pre-BötC, pre-Bötzing complex; py, pyramidal tract; scp, superior cerebellar peduncle; sp5, spinal trigeminal tract; Sp5i, spinal trigeminal nucleus pars interpositus.

of the ponto-medullary respiratory network (ventral respiratory group, Bregma  $-14.0$ ; preBötzing complex, Bregma  $-12.7$ ; parafacial region, Bregma  $-10.9$ ; A5 region, Bregma  $-10.2$  and Kölliker–Fuse nucleus, Bregma  $-9.0$ ). The coordinates refer to brainstem levels from juvenile rats according to Paxinos & Watson (2005). Regions of interest in neonatal brainstems were determined according to anatomical landmarks. Cell counts were performed in  $10\,000\ \mu\text{m}^2$  areas of these nuclei.

To assess developmental changes in NMDA currents and BDNF effects, the recorded neurones were pooled into three groups: neonatal (postnatal day P1–5), intermediate (P6–13) and juvenile (P14–21). Developmental changes in the decay kinetics of NMDA currents were analysed with MiniAnalysis (Synaptosoft Inc., Decatur, GA, USA). NMDA currents were digitally filtered (Lowpass Chebychev, cut-off frequency 50 Hz), averaged, and fitted to an exponential function of the form  $y = A1 \cdot \exp(-x/\tau_1)$ . Fitting range was from 10 to 90%. The weighted tau was calculated by normalizing to the amplitude so that the decay kinetics are expressed in milliseconds per picoamp. NMDA current amplitudes were analysed offline with Clampfit. Each trial was averaged and mean amplitudes were measured. Data are presented as (normalized) means  $\pm$  s.e.m.

### Statistical analysis

Statistical comparison of developmental changes in NR2B- and NR2D-positive neurones, NMDA amplitudes and decay kinetics between the three groups were performed with ANOVA followed by a Tukey *post hoc* test (Systat 11, Systat software, Inc. 2004). Linear regression analyses were performed with ANCOVA (Systat 11) for repetitive NMDA applications with and without pharmacological manipulations. For comparisons

between NMDA-evoked currents during control experiments and after pharmacological manipulation we used unpaired two tailed Student's *t* tests (Microsoft Excel). A *P* value  $< 0.05$  was considered as significant.

## Results

### Developmental changes in the expression profile of NMDA receptor subunit 2D (NR2D) and 2B (NR2B) in the ponto-medullary respiratory network

To test the effect of BDNF on NMDA-R-mediated postsynaptic currents, we first analysed the expression of the NMDA-R subunits NR2D and NR2B in the ponto-medullary respiratory network during postnatal development. In this and the subsequent experiments the data were pooled into three different age groups: neonatal age group (postnatal day P1–5), intermediate age group (P6–13) and juvenile age group (P14–21; see also Kron *et al.* 2007a). Quantitative analyses revealed a highly significant developmental up-regulation in the numbers of NR2D subunit expressing neurones (ANOVA,  $P < 0.001$ ; Figs 1A and 2A) in the KF. In contrast, numbers of NR2B subunit-positive neurones showed a highly significant developmental decrease (ANOVA,  $P < 0.001$ ; Figs 1A and 2B). The number of NR2D-positive neurones increased from  $8.6 \pm 0.3$  neurones  $(10\,000\ \mu\text{m}^2)^{-1}$  in the neonatal group ( $n = 7$ ) to  $13.5 \pm 1.6$  neurones  $(10\,000\ \mu\text{m}^2)^{-1}$  in the intermediate group ( $n = 8$ ) and finally to  $23.3 \pm 3.0$  neurones  $(10\,000\ \mu\text{m}^2)^{-1}$  in the juvenile group ( $n = 8$ , Fig. 2A). In contrast, the highest number of NR2B-positive neurones was observed in the neonatal KF ( $35.3 \pm 4.1$  neurones  $(10\,000\ \mu\text{m}^2)^{-1}$ ,  $n = 7$ ). With ongoing postnatal development NR2B expression progressively decreased to  $22.0 \pm 2.2$  neurones  $(10\,000\ \mu\text{m}^2)^{-1}$  in the intermediate group

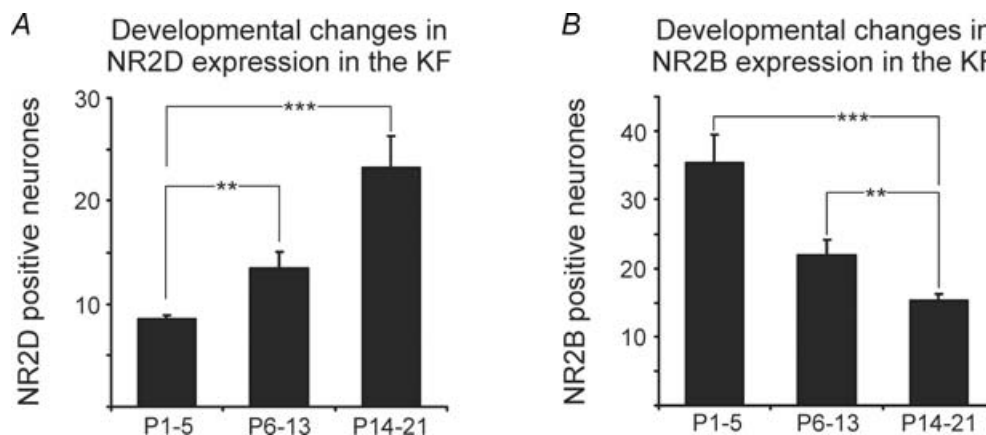


**Figure 2. Developmental changes in the expression profiles of NR2D and NR2B subunits in the KF**  
 A, developmental increase of NR2D-positive neurones in the KF. B, developmental decrease of NR2B-positive neurones in the KF. \*\* $P < 0.01$ , \*\*\* $P < 0.001$ , ANOVA with *post hoc* Tukey's test.

( $n = 8$ ) and  $15.4 \pm 1.0$  neurones ( $10\,000\ \mu\text{m}^2$ )<sup>-1</sup> in the juvenile group ( $n = 8$ , Fig. 2B).

A decrease in both NR2D and NR2B during postnatal development was observed in all other investigated respiratory-related areas, such as the ventral respiratory

group, the pre-Bötzinger complex (Fig. 1B), the parafacial region, and the A5 region (summarized in Table 1). Unfortunately, other antibodies against additional NMDA-R subunits were not suitable for analysis of early postnatal expression patterns. Nevertheless, our results demonstrate that NMDA-R are present in the KF in all stages tested.

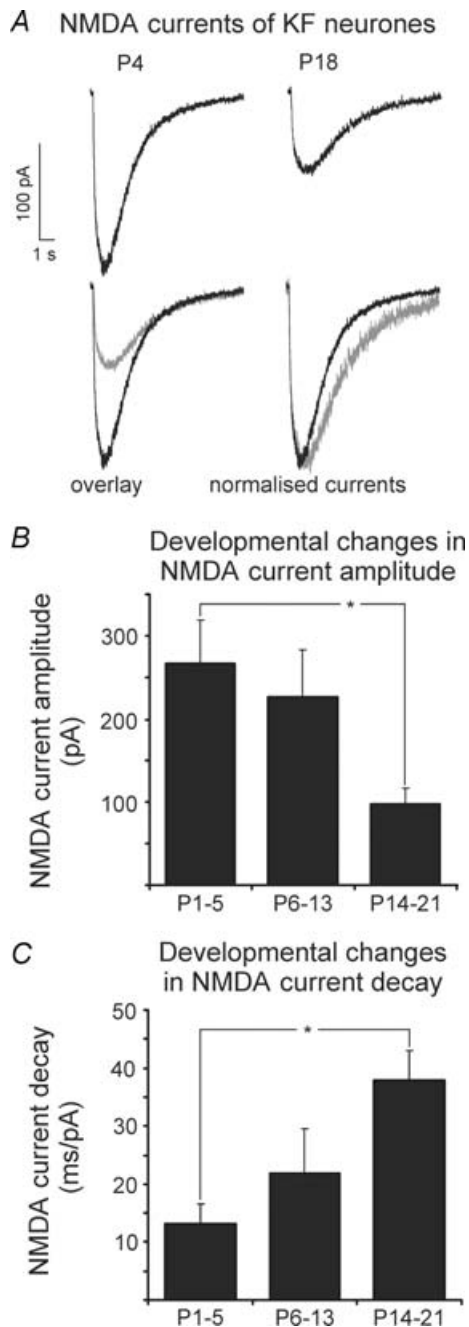


**Figure 3. Developmental changes of NMDA current characteristics in KF neurones**

A, representative recordings of NMDA currents from a neonatal and a mature KF neurone, illustrating the developmental changes in amplitude and decay time. B, developmental decrease of NMDA current amplitude. C, developmental increase of NMDA current decay time. \* $P < 0.05$ , ANOVA with *post hoc* Tukey's test.

### Developmental changes in amplitudes and decay kinetics of NMDA currents in the KF

As a next step, we analysed the function of NMDA-R by testing the agonist-evoked responses of KF neurones during postnatal development. In the neonatal age group ( $n = 7$ ), a mean amplitude of  $266.6 \pm 52.3$  pA was observed (Fig. 3A and B). NMDA currents derived from neurones of the intermediate age group ( $n = 9$ ) displayed an insignificant decrease in the mean amplitude to  $226.5 \pm 56.7$  pA (Fig. 3B). In the juvenile age group (P14–21,  $n = 11$ ) NMDA amplitudes were reduced to  $98.1 \pm 18.4$  pA (Fig. 3A and B). Statistical comparison revealed a significant difference (ANOVA,  $P < 0.05$ ) in NMDA current amplitudes between the neonatal and the juvenile age group (Fig. 3B). Analyses of NMDA current decay kinetics revealed a developmental increase in the decay time (Fig. 3A and C). In the neonatal age group we observed the fastest deactivation kinetics ( $13.1 \pm 3.4$  ms pA<sup>-1</sup>, Fig. 3C). In neurones from the intermediate age group, deactivation kinetics was slower ( $21.9 \pm 7.7$  ms pA<sup>-1</sup>, Fig. 3C). This tendency culminated in the juvenile age group, where we observed the longest decay times ( $37.9 \pm 5.1$  ms pA<sup>-1</sup>, Fig. 3C). Statistical comparison revealed a significant developmental difference (ANOVA,  $P < 0.05$ ) in the decay kinetics of NMDA currents between the neonatal and the juvenile age groups (Fig. 3C). Thus, our data suggest that developmental changes of both NMDA-R subunits in the KF (increasing NR2D, decreasing NR2B, Figs 1 and 2, Table 1), result in changes of the NMDA current characteristics.

### Developmental changes in postsynaptic responses to repetitive NMDA application on KF neurones

We next tested the postsynaptic response to brief repetitive NMDA applications on KF neurones in four consecutive trials in the three age groups (see Methods). In the neonatal group ( $n = 7$ ), the amplitude of the postsynaptic current decreased by  $-5.0 \pm 2.8\%$  ( $t = 2$  min) compared to the initial NMDA application. A further decrease in NMDA current amplitude became obvious at  $t = 10$  min ( $-14.3 \pm 4.0\%$ ) and  $t = 20$  min ( $-18.3 \pm 4.9\%$ , Fig. 4A). A similar temporal decline in the NMDA current amplitude was found in neurones from the intermediate

group (P6–13,  $n = 8$ ). NMDA current amplitude decreased by  $-3.9 \pm 3.4\%$  at  $t = 2$  min, by  $-13.5 \pm 5.6\%$  at  $t = 10$  min and finally by  $-20.8 \pm 7.7\%$  at  $t = 20$  min compared to the first NMDA application at  $t = 0$  min

(Fig. 4B). Linear regressions revealed a highly significant and progressive desensitization of the NMDA current amplitude in both groups (ANCOVA, neonatal  $P < 0.001$ , intermediate  $P < 0.01$ ).

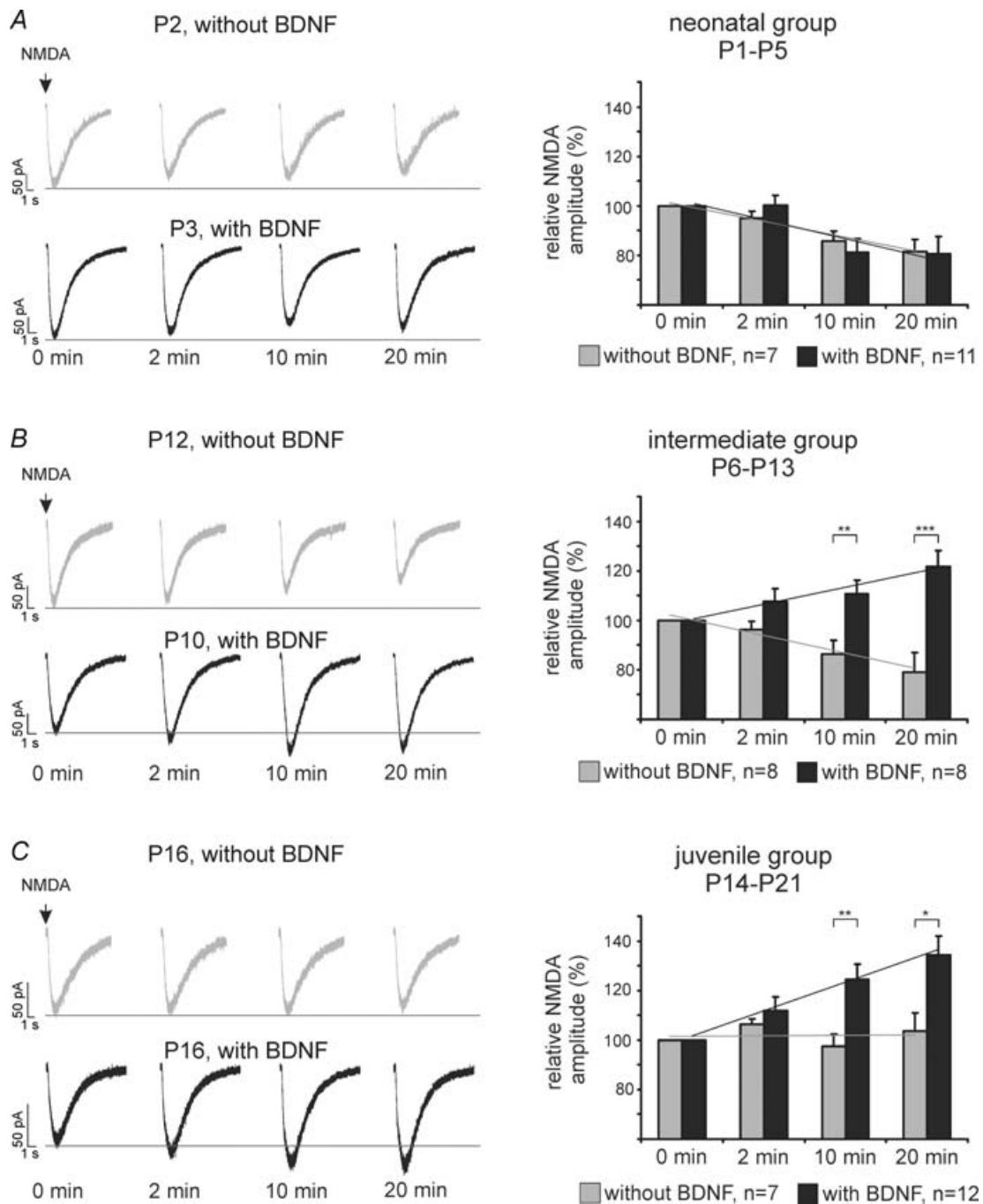


**Figure 4. Developmental differences in the postsynaptic response of KF-neurons to brief repetitive NMDA ejections with and without BDNF**

A, B and C show representative recordings (left panels) and group data (right panels) of the neonatal (A), the intermediate (B) and the juvenile group (C). The NMDA current amplitude desensitized after repetitive NMDA applications in the neonate and intermediate group (A, B) but remained unchanged in the juvenile group (C). BDNF had no effect on NMDA current amplitude in the neonatal group (A), but progressively potentiated the NMDA current amplitude in the intermediate (B) and juvenile group (C), \* $P < 0.05$ , \*\* $P < 0.01$ , \*\*\* $P < 0.001$ , unpaired two tailed Student's  $t$  tests.



In contrast, recordings from juvenile neurones (P14–21,  $n = 7$ ) showed no significant changes in the postsynaptic current amplitude in response to repetitive NMDA applications. Compared to the first ejection trials at  $t = 0$  min, NMDA amplitude increased by  $6.3 \pm 2.2\%$  at  $t = 2$  min, decreased by  $-2.4 \pm 4.9\%$  at  $t = 10$  min and remained constant at  $+3.6 \pm 7.3\%$  above the first administration after  $t = 20$  min (Fig. 4C). The subsequent analysis of linear regression revealed no significant changes of NMDA current amplitude after repetitive NMDA ejections (compare Fig. 6B). Thus, our data revealed that the changed expression of NMDA-R subunits NR2B and NR2D (Figs 1 and 2, Table 1) might also be responsible for the changed response of NMDA receptors to repetitive applications of receptor agonists.

### Developmental changes in BDNF-induced modulations of postsynaptic responses to repetitive NMDA application on KF neurones

We further investigated the effect of BDNF on NMDA-R-mediated postsynaptic responses in the KF during postnatal development. In the neonatal group (P1–5,  $n = 11$ ) BDNF showed no effects on the NMDA current amplitude compared to repetitive NMDA ejection without BDNF at all time points analysed (at 2, 10 and 20 min; Fig. 4A). Overall, NMDA currents progressively desensitized in the presence of BDNF (ANCOVA,  $P < 0.01$ ) during the repetitive ejection trials ( $t = 2$  min:  $0.0 \pm 3.9\%$ ;  $t = 10$  min:  $-18.9 \pm 5.7\%$ ;  $t = 20$  min:  $-19.4 \pm 7.0\%$ , Fig. 4A).

In the intermediate group (P6–13,  $n = 8$ ), BDNF potentiated the NMDA current amplitudes during the repetitive ejection trials. The group data revealed an increase of  $7.6 \pm 5.2\%$  of the NMDA current amplitude at  $t = 2$  min. Later, the NMDA currents showed further potentiation to  $+10.6 \pm 5.7\%$  at  $t = 10$  min and reached an increase of  $+21.8 \pm 6.3\%$  at  $t = 20$  min (Fig. 4B). Compared to control ejections without BDNF, the mean NMDA current amplitude was significantly increased at  $t = 10$  min (unpaired  $t$  test  $P < 0.01$ ) and  $t = 20$  min (unpaired  $t$  test,  $P < 0.001$ ). Linear regression revealed a significant progressive enhancement of BDNF-mediated increase of NMDA currents (ANCOVA,  $P < 0.01$ , Fig. 4B and compare Fig. 6A), while the control ejection of NMDA (without BDNF) showed a progressive desensitization (Figs 4B and 6A).

In the juvenile group, bath-application of BDNF progressively potentiated the NMDA currents in 12/18 neurones. Since the NMDA current amplitudes of 6 cells remained unchanged in the presence of BDNF, they were excluded from further analyses and were referred to as non-responsive to BDNF. The BDNF-responsive neurones showed a BDNF-mediated potentiation of NMDA

currents compared to the control experiments ( $t = 2$  min:  $+11.9 \pm 5.5\%$ , n.s.;  $t = 10$  min:  $+24.6 \pm 6.2\%$ ,  $P < 0.01$ ;  $t = 20$  min:  $+34.3 \pm 7.8\%$ ,  $P < 0.05$ , unpaired  $t$  test, Fig. 4C). Analyses of the linear regression revealed a progressive and highly significant potentiation of the NMDA current amplitude in response to BDNF application (ANCOVA,  $P < 0.001$ , compare Fig. 6B). Thus, these data demonstrate that BDNF has no effects on NMDA receptors after repetitive stimulation using the receptor agonist in the neonatal group, but progressively potentiates the NMDA receptor responses in the intermediate and juvenile groups.

### Protein kinase C (PKC) dependency of BDNF-induced potentiation of NMDA current amplitudes in KF neurones

To further investigate the intracellular signalling pathway which is involved in the BDNF-mediated potentiation of NMDA responses, the PKC dependency of the observed BDNF effects was tested in the intermediate and juvenile age groups, as BDNF only showed effects in these groups (Fig. 4).

Intracellular blockade of PKC activity by adding the PKC inhibitor peptide [19–36] to the patch clamp solution prevented the BDNF-induced potentiation of NMDA current amplitudes in the intermediate and juvenile group. After intracellular PKC blockade in the intermediate group ( $n = 10$ ), repetitive NMDA ejection revealed a slight decrease in NMDA current amplitude despite the presence of BDNF ( $t = 2$  min:  $-0.9 \pm 5.4\%$ ;  $t = 10$  min:  $-4.9 \pm 7.5\%$ ;  $t = 20$  min:  $-17.1 \pm 9.4\%$ , Fig. 5A) as was observed during control experiments without BDNF application. Linear regression revealed no progressive changes in NMDA current amplitude after PKC inhibition (ANCOVA, n.s., compare Fig. 6A). Comparative analysis with BDNF-induced modulations of NMDA current amplitudes without PKC inhibitor revealed a significant difference at  $t = 20$  min (Fig. 5A,  $P < 0.01$ , unpaired  $t$  test). The same was observed in the juvenile group (Fig. 5B,  $n = 11$ ). Regression analysis revealed no progressive changes of the NMDA current amplitudes after PKC inhibition ( $t = 2$  min:  $-0.3 \pm 4.2\%$ ;  $t = 10$  min:  $-3.5 \pm 6.1\%$ ;  $t = 20$  min:  $+3.1 \pm 8.7\%$ , Figs 5B and 6B; ANCOVA, n.s.). Comparative analysis with BDNF-induced modulation of NMDA current amplitudes without the PKC inhibitor revealed significant differences at  $t = 10$  min ( $P < 0.01$ , unpaired  $t$  test) and  $t = 20$  min ( $P < 0.05$ , unpaired  $t$  test) in the juvenile age group (Fig. 5B).

To further test whether the BDNF-mediated potentiation of NMDA currents in the intermediate and juvenile group is  $\text{Ca}^{2+}$  dependent, the effects of BDNF were studied after preincubation of the slices



with BAPTA-AM, a potent  $\text{Ca}^{2+}$  chelator. Neurones from the intermediate age group ( $n = 9$ ), incubated with BAPTA-AM, responded heterogeneously, and individual neurones still showed a moderate BDNF-mediated potentiation (see s.e.m.s below). Nevertheless, the group data revealed that the BDNF-mediated progressive potentiation of NMDA currents was abolished after BAPTA-AM loading in the intermediate age group ( $t = 2$  min:  $+3.9 \pm 7.7\%$ ;  $t = 10$  min:  $-0.6 \pm 10.8\%$ ;  $t = 20$  min:  $+3.8 \pm 11.8\%$ , Fig. 6A). In the juvenile age group ( $n = 10$ ) the effects of BAPTA-AM preincubation were comparable to PKC inhibition and no progressive potentiation was observed ( $t = 2$  min:  $-1.6 \pm 5.9\%$ ;  $t = 10$  min:  $-4.8 \pm 5.3\%$ ;  $t = 20$  min:  $-1.7 \pm 6.9\%$ , Fig. 6B, ANCOVA, n.s.). Comparative analysis with BDNF-induced modulations of NMDA current amplitudes without BAPTA-AM revealed a significant difference at  $t = 10$  min ( $P < 0.01$ , unpaired  $t$  test) and  $t = 20$  min ( $P < 0.01$ , unpaired  $t$  test) in the juvenile age group (data not shown).

## Discussion

The present study revealed a developmental decrease in NMDA current amplitudes as well as a prolongation of NMDA current decay time. These changes correlated with a developmental up-regulation of the NMDA-R subunit NR2D and a down-regulation of NR2B. Furthermore, NMDA current desensitization was only observed in immature neurones from neonatal and intermediate age groups, but was absent in mature neurones from juvenile animals. In turn, NMDA currents were progressively potentiated by BDNF in KF neurones only in intermediate and juvenile age groups, but not in neonates. The BDNF-mediated potentiation of NMDA currents could be prevented by either inhibition of protein kinase C or by  $\text{Ca}^{2+}$  chelation.

## Technical considerations

NMDA was applied exogenously on the neurones via pressure air ejections. Pipette distance (50–100  $\mu\text{m}$ ) and

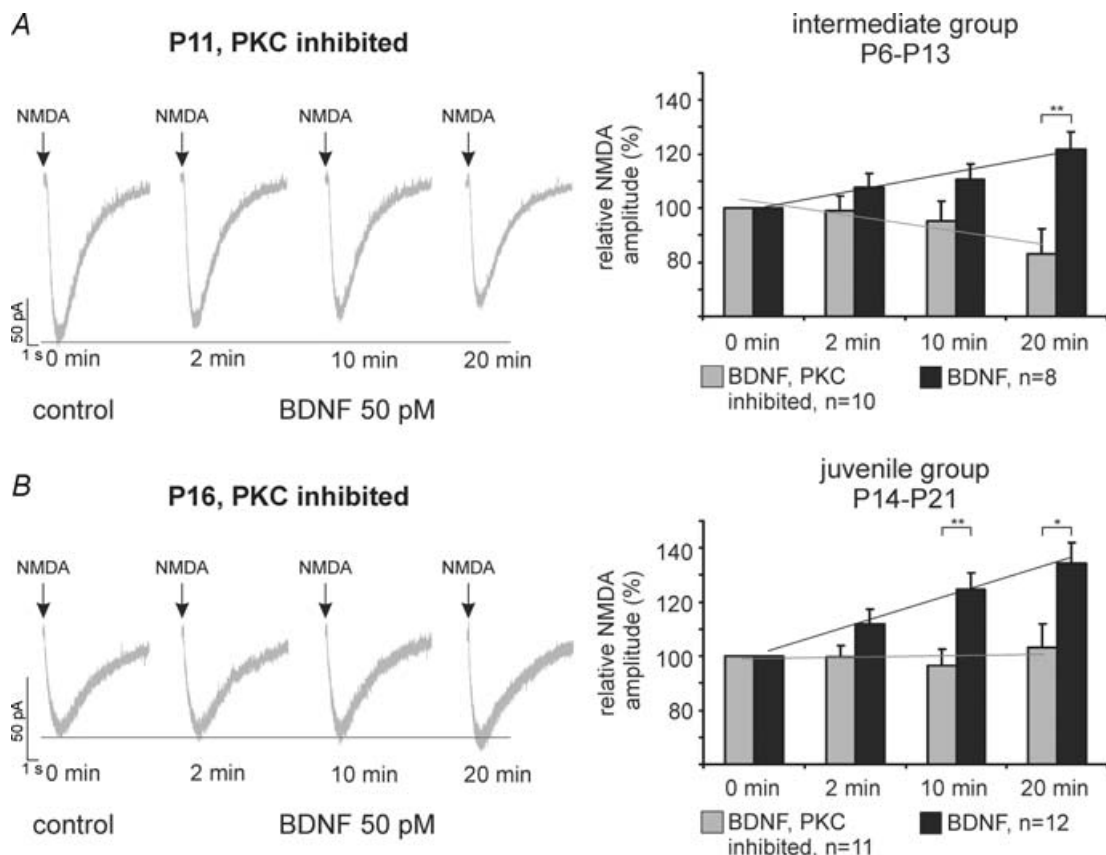


**Figure 5. BDNF-induced potentiation of NMDA current amplitude is prevented by intracellular blockade of protein kinase C**

Representative recordings (left) and group data (right) illustrate that inhibition of protein kinase C blocked BDNF-induced enhancements of the NMDA current amplitude in the intermediate (A) and juvenile group (B).

\* $P < 0.05$ , \*\* $P < 0.01$ , unpaired two tailed Student's  $t$  tests.

ejection pressure were adjusted according to the threshold of individual neurones in individual experiments. As the threshold detection method was used in every experiment, we are confident that changes of NMDA-R-mediated amplitudes are due to developmental changes in NMDA-R subunit composition and are not caused by a systematic error in the experimental approach.

It is well documented that the KF plays an essential role in the function of the respiratory network, although it is also involved in other physiological functions including cardiovascular control (Erickson & Millhorn, 1994) or nociception (Hodge *et al.* 1986; Jones, 1991; Jiang *et al.* 2004). Therefore it can not be excluded that non-respiratory-related neurones were also recorded and analysed. Nevertheless, NMDA-R-mediated neurotransmission in the KF is closely linked to the adaptation and modulation of the respiratory pattern (Bianchi *et al.* 1995; Bonham, 1995; St-John, 1998). Therefore the discussion below focuses on the potential impact of the present study on neuronal control of breathing.

### General developmental changes in NMDA-R subunit expression and NMDA-R-mediated neurotransmission in the KF

Overall, both investigated subunits (NR2B, NR2D) were down-regulated in all nuclei of the respiratory network during the postnatal development. This is in accordance with the developmental regulation of these subunits in various brain regions (Cull-Candy *et al.* 2001). However, our studies revealed an exceptional up-regulation of the NR2D subunit in the KF. The expression of NR2D subunits in functional NMDA-R is associated with low conductance and long deactivation kinetics of NMDA currents (Misra *et al.* 2000; Cull-Candy *et al.* 2001). Indeed, NMDA currents recorded from juvenile (mature) KF neurones displayed characteristic features (e.g. small amplitudes

and long decay times) which depend on the functional expression of the NR2D subunit in the NMDA-R. The lack of desensitization of NMDA currents in the juvenile age group further supports the functional expression of the NR2D subunit, since recombinant NMDA-R containing the NR2D subunit showed no desensitization during glutamate exposure (Wyllie *et al.* 1998). The physiological relevance of a functional expression of the NR2D in the KF (also see Guthmann & Herbert, 1999) may be related to a reduced  $Mg^{2+}$  block of heteromeric NMDA-R (Kuner & Schoepfer, 1996; Arvanian *et al.* 2004). The low- $Mg^{2+}$  block allows a rapid membrane depolarization of NMDA-R-mediated glutamatergic neurotransmission (Clarke & Johnson, 2006) and requires no predepolarization via AMPA/kainate receptors. This can explain previous findings, which show that blockade of NMDA-R in the KF without pharmacological manipulation of other glutamate receptor types can disrupt the respiratory pattern formation (Bianchi *et al.* 1995; Bonham, 1995; St-John, 1998) or reflex mediation (Dutschmann & Herbert, 1998; Siniiaia *et al.* 2000). Furthermore, the long deactivation kinetics of NR2D-mediated NMDA currents can result in a continuous background current (Vicini & Rumbaugh, 2000), which may provide a larger time window for activity-dependent forms of synaptic plasticity in the KF.

### BDNF-mediated postsynaptic modulation of NMDA currents in the developing KF

A BDNF-induced modulation of NMDA current amplitudes was not observed in neonatal neurones, while a significant and progressive potentiation of the NMDA current amplitudes was found in intermediate and juvenile neurones. BDNF effects are mediated by the high affinity receptor tyrosine kinase B (trkB), which is localized pre- and postsynaptically (Wu *et al.*

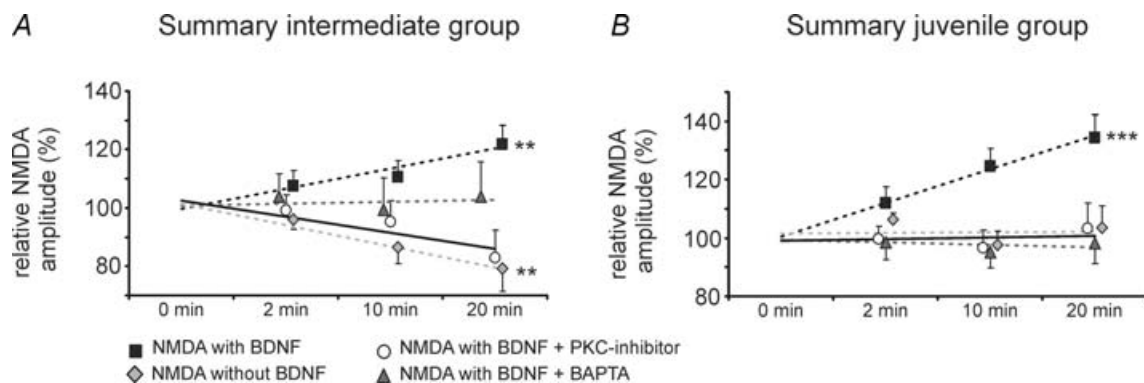


**Figure 6. Summary of BDNF-evoked potentiation of NMDA currents with and without PKC inhibition and intracellular  $Ca^{2+}$  chelation in comparison with repetitive NMDA ejection alone**

A, intermediate age group. B, juvenile age group. BDNF-induced potentiation depends on intracellular  $Ca^{2+}$  elevations and PKC activation. ANCOVA, \*\* $P < 0.01$ , \*\*\* $P < 0.001$ .

1996; Aoki *et al.* 2000; Yamada & Nabeshima, 2003). In the present study, the BDNF effects on NMDA responses were investigated in the presence of TTX, which blocked the action potential-dependent neurotransmission. Therefore, the BDNF-induced potentiation of NMDA current amplitudes most probably involves postsynaptic mechanisms, although presynaptic effects on glutamatergic neurotransmission can not be completely excluded.

In our experiments, the BDNF-induced potentiation of NMDA current amplitudes could be largely prevented by postsynaptic inhibition of protein kinase C or chelation of intracellular  $Ca^{2+}$ . PKC is particularly involved in the modulation of NMDA-R-mediated neurotransmission by different mechanisms (for review see MacDonald *et al.* 2001). It was shown that PKC increases both the NMDA channel open probability and the number of NMDA-R (Xiong *et al.* 1998; Lan *et al.* 2001), but also modulates NMDA-R via differential subunit phosphorylation (Leonard & Hell, 1997; Liao *et al.* 2001; Slack *et al.* 2004; Sanchez-Perez & Felipo, 2005). The activation of PKC itself requires intracellular  $Ca^{2+}$  elevations and the presence of diacylglycerol. Both are components of the inositoltrisphosphate ( $IP_3$ ) pathway of *trkB* signalling (Huang & Reichardt, 2001, 2003). Thus, our data suggest that the BDNF-induced potentiation of NMDA current amplitudes is linked with the activation of *trkB* and the  $IP_3$ -PKC signalling pathway. In the present study, the absence of BDNF-induced potentiation of NMDA current amplitudes in neonatal neurones coincided with the developmental up-regulation of the NR2D subunit in the KF. This raises an interesting question of whether BDNF-mediated effects on NMDA-R depend on certain NMDA-R subunits. So far, we are not aware of any experimental evidence that might answer this question.

### Physiological implications

Previously we postulated that at least specific forms of activity-dependent plasticity required for adaptation of the breathing pattern in response to peripheral or central commands are absent during early neonatal stages. Furthermore, the maturation of adaptive respiratory network function may correlate with NMDA-R-dependent plasticity in the KF (Dutschmann *et al.* 2004). The potential importance of BDNF-mediated plasticity in the KF for network function is supported by recent studies on respiratory network dysfunction in Rett syndrome (RTT, Viemari *et al.* 2005; Stettner *et al.* 2007). The RTT is a neurodevelopmental disorder associated with BDNF deficiency (Chang *et al.* 2006; Wang *et al.* 2006; Ogier *et al.* 2007). Of particular importance for the neuronal control of breathing is the BDNF deficiency within the nucleus

of the solitary tract (NTS, Wang *et al.* 2006; Ogier *et al.* 2007). The NTS as a major relay of respiratory-relevant afferent synaptic inputs is tightly connected with the KF (Herbert *et al.* 1990). These second order synapses in the KF have an important function for adaptive behaviour of the respiratory network (Song & Poon, 2004; Dutschmann *et al.* 2004). Interestingly, the investigation of the breathing dysfunction in RTT revealed a potential synaptic impairment within the KF and, more important, a lack of plasticity during NTS/KF-dependent processing of respiratory reflexes (Stettner *et al.* 2007). These findings underline the potential importance of BDNF-mediated plasticity in respiratory control in healthy and diseased states.

### References

- Akazawa C, Shigemoto R, Bessho Y, Nakanishi S & Mizuno N (1994). Differential expression of five N-methyl-D-aspartate receptor subunit mRNAs in the cerebellum of developing and adult rats. *J Comp Neurol* **347**, 150–160.
- Alheid GF, Milsom WK & McCrimmon DR (2004). Pontine influences on breathing: an overview. *Respir Physiol Neurobiol* **143**, 105–114.
- Aoki C, Wu K, Elste A, Len G, Lin S, McAuliffe G & Black IB (2000). Localization of brain-derived neurotrophic factor and *TrkB* receptors to postsynaptic densities of adult rat cerebral cortex. *J Neurosci Res* **59**, 454–463.
- Arvanian VL, Bowers WJ, Petruska JC, Motin V, Manuzon H, Narrow WC, Federoff HJ & Mendell LM (2004). Viral delivery of NR2D subunits reduces  $Mg^{2+}$  block of NMDA receptor and restores NT-3-induced potentiation of AMPA-kainate responses in maturing rat motoneurons. *J Neurophysiol* **92**, 2394–2404.
- Bianchi AL, Denavit-Saubie M & Champagnat J (1995). Central control of breathing in mammals: neuronal circuitry, membrane properties, and neurotransmitters. *Physiol Rev* **75**, 1–45.
- Bonham AC (1995). Neurotransmitters in the CNS control of breathing. *Respir Physiol* **101**, 219–230.
- Chang Q, Khare G, Dani V, Nelson S & Jaenisch R (2006). The disease progression of *Mecp2* mutant mice is affected by the level of BDNF expression. *Neuron* **49**, 341–348.
- Clarke RJ & Johnson JW (2006). NMDA receptor NR2 subunit dependence of the slow component of magnesium unblock. *J Neurosci* **26**, 5825–5834.
- Cull-Candy S, Brickley S & Farrant M (2001). NMDA receptor subunits: diversity, development and disease. *Curr Opin Neurobiol* **11**, 327–335.
- Das KP, Chao SL, White LD, Haines WT, Harry GJ, Tilson HA & Barone S Jr (2001). Differential patterns of nerve growth factor, brain-derived neurotrophic factor and neurotrophin-3 mRNA and protein levels in developing regions of rat brain. *Neuroscience* **103**, 739–761.
- Dutschmann M, Guthmann A & Herbert H (1998). NMDA receptor subunit NR1-immunoreactivity in the rat pons and brainstem and colocalization with Fos induced by nasal stimulation. *Brain Res* **809**, 221–230.

- Dutschmann M & Herbert H (1998). NMDA and GABA<sub>A</sub> receptors in the rat Kölliker-Fuse area control cardiorespiratory responses evoked by trigeminal ethmoidal nerve stimulation. *J Physiol* **510**, 793–804.
- Dutschmann M & Herbert H (2006). The Kölliker-Fuse nucleus gates the postinspiratory phase of the respiratory cycle to control inspiratory off-switch and upper airway resistance in rat. *Eur J Neurosci* **24**, 1071–1084.
- Dutschmann M, Mörschel M, Kron M & Herbert H (2004). Development of adaptive behaviour of the respiratory network: implications for the pontine Kölliker-Fuse nucleus. *Respir Physiol Neurobiol* **143**, 155–165.
- Erickson JT & Millhorn DE (1994). Hypoxia and electrical stimulation of the carotid sinus nerve induce Fos-like immunoreactivity within catecholaminergic and serotonergic neurons of the rat brainstem. *J Comp Neurol* **348**, 161–182.
- Ezure K (2004). Respiration-related afferents to parabrachial pontine regions. *Respir Physiol Neurobiol* **143**, 167–175.
- Feil K & Herbert H (1995). Topographic organization of spinal and trigeminal somatosensory pathways to the rat parabrachial and Kölliker-Fuse nuclei. *J Comp Neurol* **353**, 506–528.
- Gilmore JH, Jarskog LF & Vadlamudi S (2003). Maternal infection regulates BDNF and NGF expression in fetal and neonatal brain and maternal-fetal unit of the rat. *J Neuroimmunol* **138**, 49–55.
- Guthmann A & Herbert H (1999). Expression of N-methyl-D-aspartate receptor subunits in the rat parabrachial and Kölliker-Fuse nuclei and in selected pontomedullary brainstem nuclei. *J Comp Neurol* **415**, 501–517.
- Herbert H, Moga MM & Saper CB (1990). Connections of the parabrachial nucleus with the nucleus of the solitary tract and the medullary reticular formation in the rat. *J Comp Neurol* **293**, 540–580.
- Hodge CJ Jr, Apkarian AV & Stevens RT (1986). Inhibition of dorsal-horn cell responses by stimulation of the Kölliker-Fuse nucleus. *J Neurosurg* **65**, 825–833.
- Huang EJ & Reichardt LF (2001). Neurotrophins: roles in neuronal development and function. *Annu Rev Neurosci* **24**, 677–736.
- Huang EJ & Reichardt LF (2003). Trk receptors: roles in neuronal signal transduction. *Annu Rev Biochem* **72**, 609–642.
- Jiang M, Alheid GF, Calandriello T & McCrimmon DR (2004). Parabrachial-lateral pontine neurons link nociception and breathing. *Respir Physiol Neurobiol* **143**, 215–233.
- Jones SL (1991). Descending noradrenergic influences on pain. *Prog Brain Res* **88**, 381–394.
- Kim YI, Choi HJ & Colwell CS (2006). Brain-derived neurotrophic factor regulation of N-methyl-D-aspartate receptor-mediated synaptic currents in suprachiasmatic nucleus neurons. *J Neurosci Res* **84**, 1512–1520.
- Kron M, Mörschel M, Reuter J, Zhang W & Dutschmann M (2007a). Developmental changes in brain-derived neurotrophic factor-mediated modulations of synaptic activities in the pontine Kölliker-Fuse nucleus of the rat. *J Physiol* **583**, 315–327.
- Kron M, Zhang W & Dutschmann M (2007b). Developmental changes in the BDNF-induced modulation of inhibitory synaptic transmission in the Kölliker-Fuse nucleus of rat. *Eur J Neurosci* **26**, 3449–3457.
- Kuner T & Schoepfer R (1996). Multiple structural elements determine subunit specificity of Mg<sup>2+</sup> block in NMDA receptor channels. *J Neurosci* **16**, 3549–3558.
- Lan JY, Skeberdis VA, Jover T, Grooms SY, Lin Y, Araneda RC, Zheng X, Bennett MV & Zukin RS (2001). Protein kinase C modulates NMDA receptor trafficking and gating. *Nat Neurosci* **4**, 382–390.
- Leonard AS & Hell JW (1997). Cyclic AMP-dependent protein kinase and protein kinase C phosphorylate N-methyl-D-aspartate receptors at different sites. *J Biol Chem* **272**, 12107–12115.
- Levine ES, Crozier RA, Black IB & Plummer MR (1998). Brain-derived neurotrophic factor modulates hippocampal synaptic transmission by increasing N-methyl-D-aspartic acid receptor activity. *Proc Natl Acad Sci U S A* **95**, 10235–10239.
- Liao GY, Wagner DA, Hsu MH & Leonard JP (2001). Evidence for direct protein kinase-C mediated modulation of N-methyl-D-aspartate receptor current. *Mol Pharmacol* **59**, 960–964.
- Lin SY, Wu K, Levine ES, Mount HT, Suen PC & Black IB (1998). BDNF acutely increases tyrosine phosphorylation of the NMDA receptor subunit 2B in cortical and hippocampal postsynaptic densities. *Brain Res Mol Brain Res* **55**, 20–27.
- Lu B (2003). BDNF and activity-dependent synaptic modulation. *Learn Mem* **10**, 86–98.
- MacDonald JF, Kotecha SA, Lu WY & Jackson MF (2001). Convergence of PKC-dependent kinase signal cascades on NMDA receptors. *Curr Drug Targets* **2**, 299–312.
- Misra C, Brickley SG, Wyllie DJ & Cull-Candy SG (2000). Slow deactivation kinetics of NMDA receptors containing NR1 and NR2D subunits in rat cerebellar Purkinje cells. *J Physiol* **525**, 299–305.
- Monyer H, Burnashev N, Laurie DJ, Sakmann B & Seeburg PH (1994). Developmental and regional expression in the rat brain and functional properties of four NMDA receptors. *Neuron* **12**, 529–540.
- Ogier M, Wang H, Hong E, Wang Q, Greenberg ME & Katz DM (2007). Brain-derived neurotrophic factor expression and respiratory function improve after ampakine treatment in a mouse model of Rett syndrome. *J Neurosci* **27**, 10912–10917.
- Okazaki M, Takeda R, Yamazaki H & Haji A (2002). Synaptic mechanisms of inspiratory off-switching evoked by pontine pneumotaxic stimulation in cats. *Neurosci Res* **44**, 101–110.
- Paxinos G & Watson C (2005). *The Rat Brain in Stereotaxic Coordinates*, 5th edn. Academic Press, New York.
- St-John WM (1998). Neurogenesis of patterns of automatic ventilatory activity. *Prog Neurobiol* **56**, 97–117.
- Sanchez-Perez AM & Felipo V (2005). Serines 890 and 896 of the NMDA receptor subunit NR1 are differentially phosphorylated by protein kinase C isoforms. *Neurochem Int* **47**, 84–91.
- Sheng M & Kim MJ (2002). Postsynaptic signaling and plasticity mechanisms. *Science* **298**, 776–780.

- Siniaia MS, Young DL & Poon CS (2000). Habituation and desensitization of the Hering–Breuer reflex in rat. *J Physiol* **523**, 479–491.
- Slack SE, Pezet S, McMahon SB, Thompson SW & Malcangio M (2004). Brain-derived neurotrophic factor induces NMDA receptor subunit one phosphorylation via ERK and PKC in the rat spinal cord. *Eur J Neurosci* **20**, 1769–1778.
- Song G & Poon CS (2004). Functional and structural models of pontine modulation of mechanoreceptor and chemoreceptor reflexes. *Respir Physiol Neurobiol* **143**, 281–292.
- Stettner GM, Huppke P, Brendel C, Richter DW, Gartner J & Dutschmann M (2007). Breathing dysfunctions associated with impaired control of postinspiratory activity in *Mecp2*<sup>-/-</sup> knockout mice. *J Physiol* **579**, 863–876.
- Suen PC, Wu K, Levine ES, Mount HT, Xu JL, Lin SY & Black IB (1997). Brain-derived neurotrophic factor rapidly enhances phosphorylation of the postsynaptic N-methyl-D-aspartate receptor subunit 1. *Proc Natl Acad Sci U S A* **94**, 8191–8195.
- Takano K & Kato F (2003). Inspiration-promoting vagal reflex in anaesthetized rabbits after rostral dorsolateral pons lesions. *J Physiol* **550**, 973–983.
- Vicini S & Rumbaugh G (2000). A slow NMDA channel: in search of a role. *J Physiol* **525**, 283.
- Viemari JC, Roux JC, Tryba AK, Saywell V, Burnet H, Pena F, Zanella S, Bevengut M, Barthelemy-Requin M, Herzing LB, Moncla A, Mancini J, Ramirez JM, Villard L & Hilaire G (2005). *Mecp2* deficiency disrupts norepinephrine and respiratory systems in mice. *J Neurosci* **25**, 11521–11530.
- Wang H, Chan SA, Ogier M, Hellard D, Wang Q, Smith C & Katz DM (2006). Dysregulation of brain-derived neurotrophic factor expression and neurosecretory function in *Mecp2* null mice. *J Neurosci* **26**, 10911–10915.
- Wu K, Xu JL, Suen PC, Levine E, Huang YY, Mount HT, Lin SY & Black IB (1996). Functional trkB neurotrophin receptors are intrinsic components of the adult brain postsynaptic density. *Brain Res Mol Brain Res* **43**, 286–290.
- Wyllie DJ, Behe P & Colquhoun D (1998). Single-channel activations and concentration jumps: comparison of recombinant NR1a/NR2A and NR1a/NR2D NMDA receptors. *J Physiol* **510**, 1–18.
- Xiong ZG, Raouf R, Lu WY, Wang LY, Orser BA, Dudek EM, Browning MD & MacDonald JF (1998). Regulation of N-methyl-D-aspartate receptor function by constitutively active protein kinase C. *Mol Pharmacol* **54**, 1055–1063.
- Xu F, Plummer MR, Len GW, Nakazawa T, Yamamoto T, Black IB & Wu K (2006). Brain-derived neurotrophic factor rapidly increases NMDA receptor channel activity through Fyn-mediated phosphorylation. *Brain Res* **1121**, 22–34.
- Yamada K, Mizuno M & Nabeshima T (2002). Role for brain-derived neurotrophic factor in learning and memory. *Life Sci* **70**, 735–744.
- Yamada K & Nabeshima T (2003). Brain-derived neurotrophic factor/TrkB signaling in memory processes. *J Pharmacol Sci* **91**, 267–270.

### Acknowledgements

This study was supported by grants of the DFG – Research Center Molecular Physiology of the Brain (CMPB; W.Z.) and Bernstein Center for Computational Neurosciences (BCCN, 01GQ0432, M.D.). We thank A. Bischoff for excellent technical assistance and Dr U. Dürr for valuable suggestions on the manuscript.

### Supplemental material

Online supplemental material for this paper can be accessed at: <http://jp.physoc.org/cgi/content/full/jphysiol.2007.148916/DC1> and <http://www.blackwell-synergy.com/doi/suppl/10.1113/jphysiol.2007.148916>